BIOCHEMISTRY
including biophysical chemistry & molecular biology

Article

Selective modulation of PKC# over PKC# by curcumin and its derivatives in CHO-K1 cells

SATYABRATA PANY, Anjoy Majhi, and Joydip Das

Biochemistry, **Just Accepted Manuscript** • DOI: 10.1021/acs.biochem.6b00057 • Publication Date (Web): 17 Mar 2016

ACS Publications

Biochemistry is published by the American Chemical Society. 1155 Sixteenth Street N.W., Washington, DC 20036

Selective modulation of PKCα over PKCε by curcumin and its derivatives in CHO-K1 cells

Satyabrata Pany, Anjoy Majhi and Joydip Das*

Department of Pharmacological and Pharmaceutical Sciences, College of Pharmacy, University of Houston, Houston, TX 77204

*To whom correspondence should be addressed: Tel: 713-743-1708, Fax: 713-743-1884, Email: jdas@uh.edu.

Abstract

The protein kinase C (PKC) family of serine/threonine kinases regulate various cellular functions, including cell growth, differentiation, metabolism, and apoptosis. Modulation of isoform-selective activity of PKC by curcumin (**1**), the active constituent of *Curcuma* L., is poorly understood and the literature data is inconsistent and obscure. Effect of curcumin (**1**) and its analogs, 4-((2Z,6E)-3-hydroxy-7-(4-hydroxy-3-methoxyphenyl)-5-oxohepta-2,6-dien-1-yl)-2-methoxyphenyl oleate **(2),** (9Z,12Z)-4-((2Z,6E)-3-hydroxy-7-(4-hydroxy-3-methoxyphenyl)-5-oxohepta-2,6-dien-1-yl)-2-methoxyphenyl octadeca-9,12-dienoate **(3),** (9Z,12Z,15Z)-4-((2Z,6E)-3-hydroxy-7-(4-hydroxy-3-methoxyphenyl)-5-oxohepta-2,6-dien-1-yl)-2-methoxyphenyl octadeca-9,12,15-trienoate **(4),** and (1E,6E)-1-(4-(hexadecyloxy)-3-methoxyphenyl)-7-(4-hydroxy-3-methoxyphenyl)hepta-1,6-diene-3,5-dione (**5**) and didemethylcurcumin (**6**) on the membrane translocation of PKCα, a conventional and PKCε, a novel PKC has been studied in CHO-K1 cells, in which these PKC isoforms are endogenously expressed. Translocation of PKC from cytosol to membrane was measured using immunoblotting and confocal microscopy. **1** and **6** inhibited the TPA-induced membrane translocation of PKCα but not of PKCε. Modification of the hydroxyl group of curcumin with long aliphatic chain containing unsaturated double bonds in **2-4** completely abolished this inhibition property. Instead, **2-4** showed significant translocation of PKCα, but not of PKCε to the membrane. No membrane translocation was observed with **1**, **6** or with the analog **5** having saturated long chain for either PKCα or PKCε. **1** and **6** inhibited TPA-induced activation of ERK1/2 and **2-4** activated it. ERK1/2 is the downstream readout of PKC. The present results show that the hydroxyl group of curcumin is important for PKC activity and curcumin template can be useful in developing isoform specific PKC modulators for regulating a particular disease state.

Keywords: Curcumin, protein kinase C, phorbol ester, diacylglycerol, isoform, membrane.

Abbreviations: PKC, protein kinase C; DAG, diacylglycerol; TPA, 12-O-tetradecanoylphorbol-13-acetate; ERK, extracellular signal regulated Kinase; CHO, Chinese hamster ovary; DOG, *sn*-1,2-dioctanoylglycerol; PC, phosphatidylcholine; PS, phosphatidylserine; NMR, nuclear magnetic resonance; MTT, 3-(4,5-dimethylthiazol-2-yl)-2,5-diphenyltetrazolium bromide; ES-MS, electrospray mass spectrometry; FBS, fetal bovine serum; DMF, dimethylformamide; DMSO, dimethyl sulfoxide; SDS-PAGE, sodium dodecyl sulfonate- polyacrylamide gel electrophoresis; HRP, horseradish peroxidase; ECL, enhanced chemiluminescence; clog P, calculated value of logarithm of the partition coefficient for *n*-octanol/water; BSA, bovine serum albumin; DPPH, 2, 2-diphenyl-1-picrylhydrazyl; FITC, fluorescein isothiocyanate.

Protein kinase C (PKC) is a family of serine/threonine protein kinases involved in the regulation of various aspects of cell functions, including cell growth, differentiation, metabolism, and apoptosis(*1*). Its role has been implicated in the pathology of several diseases such as cancer, diabetes, stroke, heart failure, and Alzheimer's disease (*2-8*). PKC has been a subject of intense research and drug development for these disease states (*9, 10*).

The PKC family has been divided into three main groups: conventional isoforms (α, βI, βII and γ) that require Ca^{2+} and diacylglycerol (DAG) for activation; novel isoforms (δ, ε, η, θ and μ) that require only DAG and atypical isoforms (ζ, ι and λ) that require neither Ca^{2+} nor DAG(*11*). DAG is generated by the phospholipase C-catalyzed hydrolysis of membrane phosphatidylinositol-4,5-bisphosphate (PIP_2). It contains two long chains and acts as a second messenger(*12*). These two acyl chains remain embedded in the membrane during the PKC activation process. DAG interacts with proteins containing a C1 domain and induces their translocation to discrete subcellular compartments. In the conventional and novel PKC isoforms, the DAG-sensitive C1 domain is duplicated into a tandem C1 domain consisting of C1A and C1B subdomains. Along with the PKC family, there are about six additional families of proteins that contain a DAG-responsive C1 domain (*13, 14*).

Naturally occurring tumor-promoters, phorbol esters also bind to the C1 domain and actually activates PKC several fold higher than the endogenous DAG (*15, 16*). In addition, several other naturally occurring compounds including bryostatins, teleocidins, aplysiatoxins, ingenols, and iridals bind to the C1 domain. However, most of the naturally occurring C1 domain ligands are highly complex in their structure and show very poor or no isoform specificity (*17, 18*). Therefore, structural modification with the aim of altering the ligand specificity has been difficult. Moreover, many of these ligands are associated with toxicity problems. To circumvent these problems, the strategy has been to find simpler template for ligand synthesis, whose structure could be easily modified and fine-tuned in order to achieve selectivity and expected to be non-toxic.

Curcumin (**1, Fig. 1**) is a β-diketone constituent of turmeric obtained from the powdered root of *Curcuma* L. (*19, 20*). Not only is it used as a spice to give a specific flavor and yellow

color to curry, which is consumed in trace quantities daily by millions of people, curcumin has also been used as a traditional medicine for liver disease (jaundice), indigestion, urinary tract diseases, rheumatoid arthritis, and insect bites (*19-21*). Curcumin is a promising therapeutic agent for diseases such as cancer, diabetes, multiple sclerosis, Alzheimer's, HIV and cardiovascular disease (*22-24*).

The positive interference of curcumin with the tumor promoting effects of phorbol esters has been attributed to its effect on the phorbol ester receptor, protein kinase C (PKC)(*25*) (*26-28*). There are well-documented studies on the modulation of PKC activity by curcumin *in vivo* (*29, 30*) and *in vitro* (*31, 32*). However, the mechanism by which curcumin modulates PKC activity is poorly understood. In studies involving purified proteins, curcumin (< 20 μM) was shown to activate PKCα in the presence of membrane(*32*). At higher curcumin concentration (> 20 μM), decrease in activity was observed. In another study using purified protein it was also shown that curcumin (6-48 μM) activated calcium sensitive PKC (e.g. PKCα) in the presence of membrane and inhibited it in the absence of membrane(*31*). Similarly, another study showed that in a membrane-free system, curcumin (100 μM) inhibited PKC(*30*). All these results indicated that membrane, Ca^{++} and curcumin concentration are important determinants for curcumin to behave as an activator or inhibitor. Studies using cultured NIH3T3 fibroblasts have shown that curcumin (15-20 μM) alone did not affect PKC activity but it inhibited the TPA-induced PKC activity(*29*). Another study involving mouse skin showed that curcumin (10 μmol) inhibited TPA-induced membrane translocation of both PKCα and PKCε (*33*).

In our previous studies (*34, 35*) we found that addition of long chains in curcumin structure modified their binding to the C1 domains of PKCs. In this paper we describe the chemical modification of curcumin with long aliphatic chain with varying number of unsaturated double bonds on the membrane translocation properties of PKCs in CHO-K1 cells. Our results indicate that curcumin inhibited the TPA-induced PKC activity of PKCα but not PKCε. On the other hand, the long chain derivatives containing unsaturated double bonds directly activated PKCα but not PKCε.

Experimental Procedures

General

Curcumin and TPA were from Sigma. 1,2-dioctanoyl-*sn*-glycerol (DOG) was purchased from Avanti polar lipids. All other reagents were from Aldrich and used without further purification. Progress of chemical reaction was monitored through thin layer chromatography (TLC) on pre-coated glass plates (silica gel 60 F254, 0.25mm thickness) purchased from EMD chemicals. ^{1}H NMR and ^{13}C NMR spectra were recorded on a QE-300 spectrometer. Unless otherwise specified, all NMR spectra were obtained in deuterated chloroform ($CDCl_3$) and referenced to the residual solvent peak. Chemical shifts are reported in parts per million, and coupling constants in hertz (Hz). Multiplicities are reported as follows: s (singlet), d (doublet), t (triplet), m (multiplet) and br (broadened). Mass spectra were obtained on either a VG 70-S Nier Johnson or JEOL Mass Spectrometer.

Synthesis of the curcumin derivatives

For compounds **2-4**, the corresponding acid chlorides (oleic, linoleic and linolenic acid) were prepared by treatment of the acid (1 equivalent) in anhydrous dichloromethane and thionyl chloride (1.1 equivalents) under nitrogen at 0 °C with catalytic amount DMF. Acid chloride was distilled under vacuum and used immediately for the next step. Curcumin (1 equivalent) was dissolved in anhydrous pyridine at 0 °C under nitrogen and treated with different acid chlorides. The reaction mixture was allowed to stirring for 2 h at room temperature and then heated at 60 °C for another 2 h. After cooling the mixture to room temperature, excess pyridine was evaporated under high vacuum. The resulting residue was subjected to column chromatography. Compounds **5** and **6** were synthesized as described earlier (*34*). The chemical structure of **1-6** is shown in Fig.1.

4-((2Z,6E)-3-hydroxy-7-(4-hydroxy-3-methoxyphenyl)-5-oxohepta-2,6-dien-1-yl)-2-methoxyphenyl oleate **(2):** Yield: 65% ^{1}H NMR (CD_3OD) δ 7.59 (2H, d, J = 16.0 Hz), 7.15-7.06 (3H, m), 7.02 (1H, d, J = 8.0 Hz), 6.91 (1H, d, J = 8.0, Hz), 6.51 (1H, d, J = 15.4 Hz), 6.47 (1H, d, J = 15.4 Hz), 6.0 (1H, brs), 5.81 (1H, s), 5.35 (2H, m), 3.91 (3H, s), 3.85 (3H, s), 2.58 (2H, t, J = 7.7 Hz), 2.01 (4H, m), 1.75 (2H, m), 1.42-1.26 (20H, m), 0.87 (3H, t, J = 6.9 Hz); ^{13}C NMR (CD_3OD) δ 184.6, 181.9, 171.9, 151.4, 148.0, 146.9, 141.3, 141.2, 139.5, 134.0, 130.1, 129.8,

127.5, 124.1, 123.3, 123.1, 121.7, 121.0, 114.9, 111.4, 109.7, 101.7, 56.0, 55.9, 34.1, 32.0, 29.8, 29.8, 29.6, 29.4, 29.2, 29.2, 29.1, 27.3, 27.2, 25.0, 22.8, 14.2; ES-MS: 633 [M+H], 655 [M+Na].

(9Z,12Z)-4-((2Z,6E)-3-hydroxy-7-(4-hydroxy-3-methoxyphenyl)-5-oxohepta-2,6-dien-1-yl)-2-methoxyphenyl octadeca-9,12-dienoate **(3):** Yield: 69% ^{1}H NMR (CD_3OD) δ 7.59 (2H, d, *J* = 15.5 Hz), 7.16-7.10 (3H, m), 7.04 (2H, d, *J* = 8.0 Hz), 6.93 (1H, d, *J* = 8.0, Hz), 6.53 (1H, d, *J* = 16.0 Hz), 6.49 (1H, d, *J* = 16.0 Hz), 5.92 (1H, brs), 5.82 (1H, s), 5.35 (4H, m), 3.93 (3H, s), 3.85 (3H, s), 2.77 (2H, t, *J* = 6.3 Hz), 2.58 (2H, t, *J* = 7.4 Hz), 2.05 (4H, m), 1.76 (2H, m), 1.48-1.29 (14H, m), 0.88 (3H, t, *J* = 6.8 Hz); ^{13}C NMR (CD_3OD) δ 184.5, 181.9, 171.8, 151.5, 148.0, 146.8, 141.2, 141.0, 139.5, 134..0, 130.3, 130.1, 128.1, 127.9, 127.6, 124.2, 123.3, 123.0, 121.8, 121.0, 114.9, 111.4, 109.7, 101.6, 56.0, 55.9, 34.1, 31.9, 29.7, 29.4, 29.2, 29.2, 27.2, 25.7, 25.0, 22.3, 14.1; ES-MS: 630 [M^+], 631 [M+H].

(9Z,12Z,15Z)-4-((2Z,6E)-3-hydroxy-7-(4-hydroxy-3-methoxyphenyl)-5-oxohepta-2,6-dien-1-yl)-2-methoxyphenyl octadeca-9,12,15-trienoate **(4):** Yield: 58% ^{1}H NMR (CD_3OD) δ 7.6 (2H, d, *J* = 15.4 Hz), 7.18-7.10 (3H, m), 7.04 (2H, d, *J* = 8.0 Hz), 6.93 (1H, d, *J* = 8.0, Hz), 6.54 (1H, d, *J* = 15.4 Hz), 6.48 (1H, d, *J* = 15.4 Hz), 5.87 (1H, brs), 5.82 (1H, s), 5.36 (6H, m), 3.94 (3H, s), 3.86 (3H, s), 2.80 (4H, t, *J* = 6.3 Hz), 2.58 (2H, t, *J* = 7.3 Hz), 2.07 (4H, m), 1.76 (2H, m), 1.45-1.35 (8H, m), 0.96 (3H, t, *J* = 7.1 Hz); ^{13}C NMR (CD_3OD) δ 184.5, 181.9, 171.8, 151.4, 148.0, 146.8, 141.3, 141.2, 139.5, 134.0, 132.0, 130.3, 128.3, 128.3, 127.8, 127.6, 127.1, 124.2, 123.3, 123.1, 121.8, 121.0, 114.9, 111.4, 109.7, 101.6, 56.0, 55.9, 34.1, 29.6, 29.2, 29.2, 29.1, 27.3, 25.7, 25.6, 25.0, 20.6, 14.3; ES-MS: 628 [M^+], 629 [M+H].

Absorption and fluorescence measurement: Ultraviolet-visible absorption and fluorescence emission spectra of curcumin (**1**) and its derivatives (**2-6**) (1-10 μM) were recorded and analyzed as described earlier (*36*).

DPPH free radical scavenging activity: Antioxidant activity of the compounds was measured using DPPH (2, 2-diphenyl-1-picrylhydrazyl) radical scavenging assay. For scavenging experiments, DPPH (60 μM) and varying concentration of compounds (0.25–60 μM) were incubated in a methanolic solution for 2 h at 25 °C. DPPH absorbance spectra were recorded

from 400 to 600 nm. The percentage of inhibition of DPPH radical by each compound was calculated using formula: $(1-F/F_0)$ x100 and plotted against concentration, where F and F_0 represented the absorbance intensity at 517 nm in the presence and in the absence of **1-6**, respectively. IC_{50} was measured from the fitted curve using Hill equation in Sigma Plot 11 (Systat Software Inc., San Jose, CA).

Cell culture: Ham's F12 medium (Life Technologies, Grand Island, NY) supplemented with fetal bovine serum (10 %), penicillin (100 units/ml) and streptomycin (100 μg/ml) were used to culture CHO-K1 cells. Cultures were maintained in humidified atmosphere containing 5% CO_2 at 37°C. Cells were starved in media without FBS for 12 h before treating with the compounds.

Cytotoxicity assays: Cytotoxicity assays were performed using Vybrant® MTT cell proliferation assay kit (Molecular Probes, Waltham, MA) as described earlier (*36*).

Cell lysis, sub-cellular fractionation and Western blotting: Whole cell, cytosolic and membrane lysates were prepared for Western blot analysis as described earlier (*36*). Briefly, cells were harvested and lysed in lysis buffer (Cell Signaling, Danvers, MA) for whole cell lysates preparation. Cell lysates (25 μg protein/lane) were subjected to SDS-PAGE and and immunoblot to detect PKCα, PKCε and ERK1/2. For detecting PKCε and PKCα in cytosolic and membrane lysates, cells were lysed in buffer containing 20 mM Tris-HCl, pH 7.4 and protease inhibitor. Lysates were then centrifuged at 40,000 rpm for 2 h at 4 °C to separate out cytosolic (supernatant) and membrane (pellet) fractions. Protein concentration of lysates were measured and subjected to SDS-PAGE (7%). Proteins in lysates were detected using standard Western blot methods and protein specific antibodies. Following antibody dilutions were used for detection: anti-rabbit PKCα, 1:500; anti-rabbit PKCε, 1:500; anti-rabbit ERK1/2, 1:1000; anti-rabbit pERK1/2, 1:500; anti-rabbit β-actin, 1:2000 and anti-rabbit HRP-conjugated, 1:5000 (Cell Signaling, Danvers, MA)

Confocal microscopy: CHO-K1 cells were cultured and treated on glass coverslips (VWR, Atlanta, GA). Cells were then fixed in PBS containing 4% paraformaldehyde on ice for 10 min. Fixed cells were rinsed in PBS at room temperature followed by incubation in PBS containing

10% normal Goat Serum and 0.1 % Triton X-100 to block the cells. The cells were then incubated with anti-PKCα antibody (dilution, 1:100) for overnight at 4 °C in blocking solution. Cells were rinsed three times in PBS and then incubated in FITC-conjugated goat anti-rabbit secondary antibody (Santa Cruz Biotechnology, Dallas, TX) (dilution, 1:200) for 1 h and visualized in Leica SP8 confocal microscope (Leica Microsystems Inc, Buffalo Grove, IL). The sub-cellular distributions of PKCα in confocal images were quantified using ImageJ software (http://rsb. info.nih.gov/ij/) (*37*) using the guidelines described earlier (*38*). Briefly, cytosol and plasma membrane (~300 nm inside the cell edge) regions were defined and their respective total fluorescence intensity was measured. The normalized intensity ratio between the cytosol and plasma-membrane are displayed in the figures.

Statistical Analysis: Statistical analyses were performed using Sigma Plot 11 and were based on three independent experiments. The results were expressed as the mean ± SEM. Statistical significance was established by one-way RM-ANOVA, followed by Bonferroni *post hoc* test. A value of $P < 0.05$ was considered significant.

Results

Absorption and emission properties of 1-6: Table S1 lists the absorption and emission maxima of curcumin (**1**) and its derivatives (**2-6**) in various solvents**.** The representative absorption spectra of **3** in different solvents are shown in Fig S1A. Absorption maxima of curcumin (**1**) in hexane and water were 404 nm and 425 nm, respectively, showing a ~20 nm red shift in polar solvent compared to the non-polar solvent. Addition of a long aliphatic chain containing unsaturated double bond caused significant blue shift of absorption maxima of the derivatives **2**-**4** compared to curcumin in water, ethanol and acetonitrile. The extent of the blue shift in acetonitrile was less compared to water and ethanol. In hexane, no significant changes were observed in the absorption maxima for the derivatives **2-5**. Also there were no significant differences in the absorption maxima with the increase in the number of double bonds in the aliphatic chain in **2-4**.

Curcumin (**1**) and its derivatives (**2-6**) also showed significant solvent-dependent change in fluorescence emission maxima (Table S1, Fig S1B). Emission maxima for curcumin in hexane

and water are 474 nm and 572 nm respectively, showing a ~100 nm red shift in polar solvent compared to the non-polar solvent. Similar red shift was also observed for compounds **2-4.** The extent of red shift increased with the increasing number of double bonds in the aliphatic chain. However, as compared to curcumin, the emission maxima of **2-4** were blue-shifted in ethanol and red-shifted in acetonitrile. No significant differences were observed between curcumin and the derivatives **2-4** in either hexane or in water.

Antioxidant properties of 1-6: Antioxidant activity of curcumin (**1**) and derivatives (**2-6**) was measured using DPPH free radical scavenging assay (Fig 2). Curcumin, with two phenolic OH groups, exhibited DPPH radical scavenging activity with an IC_{50} value of 14.7±1 μM, a value which was reported earlier (*39*). Derivative **6,** with four phenolic OH groups, showed increased DPPH radical scavenging activity with an IC_{50} value of 2.6±1μM. In contrast, derivatives **2-4**, with one phenolic OH group, showed reduced DPPH radical scavenging activities. The IC_{50} values of **2**, **3** and **4** were 20.8±1, 26.2±1, and 25.8±1 μM respectively. We did not observe any DPPH radical scavenging activity by **5.** This could be, in part, due to the poor solubility of derivative **5** in methanolic solution.

Effect of 1-6 on cell viability: Curcumin exerts cell toxicity to cancer and non-cancer cell lines (*40-42*). In the present study, we examined the toxicity by measuring the viability of CHO-K1 cells in the presence of curcumin and its derivatives (Fig 3). Curcumin (**1**) and didemethylcurcumin (**6**) showed a dose-dependent decrease in cell viability. In contrast, derivatives (**2-4**) with C_{18} unsaturated chain and derivative (**5**) C_{16} saturated alkyl chain showed higher cell viability than curcumin. Additionally, no significance difference in cell viability was observed for **2-5**.

Effect of 1-6 on PKC expression: We examined the effect of curcumin (**1**) and its derivatives (**2-6**) on the expression of PKCα and PKCε from whole cell lysate after treating CHO-K1 cells with (**1-6**, 10 μM) for 24 h (Fig 4). Curcumin (**1**) has no effect on PKCα and PKCε expression. While the expression level remains unchanged for PKCα and PKCε with C16 saturated alkyl chain derivative (**5**), the derivatives **2-4**, with C18 unsaturated aliphatic chain significantly increased the expression of PKCα, but not PKCε. The increment was calculated to be 27%,

36%, and 45% (P <0.05) for **2**, **3** and **4** respectively. For didemethylcurcumin (**6**), the expression level was significantly decreased for both PKCα and PKCε.

Effect of 1-6 on TPA-induced membrane translocation of PKCα and PKCε: TPA is a highly potent PKC activator that causes translocation of PKC from cytosol to membrane. To find out if chemical modifications of curcumin could affect PKC activity, we examined the effect of **1-6** on TPA-induced PKC membrane translocation. For this, CHO-K1 cells were co-treated with TPA (100 nM) and **1-6** (6.25-25 μM) for 1 h and distribution of PKC in cytosol and membrane was analyzed. TPA alone localized both PKCα and PKCε to membrane as expected (Fig 5). However, when curcumin was co-treated with TPA, the amount of PKCα in the membrane was reduced (P <0.05). This reduction was dose-dependent. At the same concentration curcumin alone did not affect level of PKCα in the membrane. These results were further supported by confocal analysis which showed significant increase in cytosolic to membrane ratio (P <0.05) of PKCα on co-treatment as compared to TPA alone. In contrast, the amount of PKCε in the membrane fractions remained unchanged with the co-treatment of TPA and curcumin (Fig 6). Moreover, co-treatment of **2-5** with TPA did not reduce membrane translocation of either PKCα or PKCε (Fig S2), even after raising the concentration to as high as 100 μM. Like curcumin, didemethylcurcumin (**6)** inhibited TPA-induced membrane translocation of PKCα in a dose-dependent manner, but, not of PKCε (Fig S3). In summary, curcumin and didemethylcurcumin inhibited TPA-induced membrane translocation of PKCα and this property was lost when the chemical modification was done with the addition of long aliphatic chain in **2-5**.

Effect of 1-6 on the membrane translocation of PKCα and PKCε:

The results from the previous section that the curcumin derivatives **2-5** are ineffective in inhibiting the TPA-induced membrane translocation unlike curcumin and didemethylcurcumin, we decided to check their effect on membrane translocation in the absence of TPA. Initially this experiment was performed with 1 h incubation of **1-6** with a concentration varying in the range 0-100 μM and no membrane translocation of either PKCα or PKCε was observed. Control experiments with PKC activators TPA (100 nM) and DOG (1μM) however translocated both the PKC isoforms to the membrane as expected (Fig. S4).

We then examined the effect of **1-6** on membrane translocation for 24 h incubation at 10 μM (Fig.7). At this concentration curcumin (**1**) and its analogs **5** and **6** did not cause membrane translocation of PKCα. In contrast, **2**, **3** and **4** resulted in 46%, 27% and 36% ($P< 0.05$) increase in PKCα membrane translocation, respectively. No effect on PKCε membrane translocation was observed as cytosolic and membrane fractions remain same for any of the treated compound like untreated cells. To summarize, curcumin with unsaturated aliphatic chains selectively activates/translocate PKCα over PKCε.

Effect of 1-4 and 6 on ERK1/2 phosphorylation:

To examine if inhibition/activation of PKCα by **1-4** and **6**, is propagated along the signal transduction pathway, their effect on the downstream ERK1/2 was studied. Inhibition/activation of ERK1/2 was determined by the extent of its phosphorylation in response to **1-4** and **6**. As expected, cell treated with TPA (100 nM) significantly (>2 folds) increased the level of pERK1/2 indicating activation of ERK1/2. In contrast, no effect of curcumin was observed on basal pERK1/2 level at 25 μM (Fig. 8A). However, when cells were co-treated with TPA (100 nM) and curcumin (25 μM), TPA-induced pERK1/2 level was reduced (2 fold), which is consistent with the inhibition of TPA-induced membrane translocation by curcumin. Likely, derivative **6** also inhibited TPA induced ERK1/2 phosphorylation (Fig 8B). In contrast, treatment of CHO-K1 cells with curcumin derivatives **2-4** for 24 h significantly ($P <0.05$) increased the pERK1/2 level, which again is consistent with our membrane translocation data for PKCα (Fig. 8C).These results indicated that curcumin derivatives activated the ERK1/2 pathway by presumably activating PKCα.

Discussion

Current literature data on the modulation of isoform-selective PKC activity by curcumin is obscure and inconsistent. This is, in part, due to the variation in the assay system and the purity of PKC used by different groups. In the present study we selected a simple system of CHO-K1 cells in which PKCα, a conventional PKC and PKCε, a novel PKC are endogenously expressed. Expression of these two PKC isoforms was higher than the other isoforms such as, PKCβ and

PKCθ (data not shown). We chose to measure the effect of curcumin and its derivatives on PKC using membrane translocation assay, because in its mechanism of function, PKC first translocates to the membrane from cytosol, binds to the endogenous DAG and then phosphorylates target proteins (*43*). Our results show that curcumin by itself does not affect the membrane translocation of either PKCα or PKCε, but inhibits the TPA-induced membrane translocation of PKCα, and not PKCε. Further, to elucidate the role of the hydroxyl group of curcumin, we made analogs **2-5** by modifying one of its hydroxyl groups with long aliphatic chain having varying degree of unsaturation and analog **6** in which number of hydroxyl group was increased to four from two in curcumin, and measured their effects on membrane translocation. The modification with the long aliphatic chain was done because both endogenous DAG and most potent phorbol ester, TPA contain long aliphatic chain(*43*). It was observed earlier that addition of aliphatic chains in the structure of PKC activators such as benzolactams at different positions could modify their binding to PKCs (*44, 45*). Our results show that modification of the hydroxyl group of curcumin in **2-5** completely abolished inhibition of TPA-induced membrane translocation shown by curcumin for PKCα. Instead, the derivatives with unsaturated long aliphatic chain (**2-4**) showed activation of PKCα, but not PKCε at a concentration of 5-10 μM, indicating selectivity of curcumin and its derivatives for PKCα over PKCε.

Our earlier studies with another polyphenol, resveratrol showed similar selectivity towards PKCα over PKCε in cellular environment (*36, 46*). The only difference was the extent of activation observed for the long chain derivatives with varying number of unsaturated double bonds. Whereas in the case of resveratrol, the derivative with three double bonds in the long chain (linolenic acid) caused highest membrane translocation of PKCα, the curcumin derivatives with one double bond (oleic acid) in the long chain caused highest translocation of PKCα. Derivatives with two and three double bonds in the aliphatic chain also showed substantial extent of membrane translocation. The relative extent of PKCα translocation caused by the curcumin derivatives **2-4** is similar to the extent of membrane translocation caused by the respective fatty acid chains in these derivatives, which follows the order: oleic acid ≈ linolenic acid >> linoleic acid (*36*). This also indicates that in derivatives **2-4**, the fatty acid component of the molecule

dictates its activation property rather than the curcumin moiety. In terms of selectivity, our results are also consistent with an early report that oleic acid, linoleic acid and linolenic acid cause the membrane translocation of PKCγ, a Ca^{+2}-dependent PKC, but not of PKCε (*47*).

Several studies suggested that phenolic group substituted curcumin analogs often showed aberrant or loss in cytotoxicity, which was dependent on the size and nature of the substituted group. For example, modifications of curcumin with electron donating in the ring showed less toxicity towards cancer cells (*48, 49*). Consistent to this, compounds **2-5** in which phenolic group was modified, displayed reduced cytotoxicity. The logP value is also an important factor for polyphenol cytotoxicity(*50*). For example, curcumin is more cytotoxic with log P value of 2.5 compared to bis-eugenol (a curcumin related compound) with log P value 4.8(*51*). A recent study also found a correlation between logP values of several curcumin analogs and the cellular uptake efficiency in several cancer cell lines (*39*). Our observation that the chemical modifications on the phenolic OH group of curcumin increased the logP values of **2-5** significantly (Table S1) and reduced cytotoxicity, suggests that lipophilicity of curcumin derivatives has an effect on the viability of CHO-K1 cells.

Our result that derivatization of the hydroxyl group completely reversed the modulation properties highlights the role of the hydroxyl group of curcumin in PKC modulation. Interestingly, these phenolic OH groups are also important for curcumin's antioxidant (*39, 52*) and cytotoxic properties(*48*).Consistent with this, when one of the phenolic hydroxyl groups was modified in **2-5**, antioxidant activity was reduced and these compounds did not inhibit TPA-induced membrane translocation at all. Compound **6** with four hydroxyl groups, on the other hand, showed similar membrane translocation and ERK1/2 phosphorylation property like curcumin although it shows five times more antioxidant activity as compared to curcumin. This indicates that antioxidant property of the compound does not have direct correlation with its PKC activity.

Where is the site of action of curcumin in PKC? That curcumin inhibits the TPA-induced membrane translocation of PKCα, it is tempting to suggest that curcumin competes with phorbol ester for binding to this isoform. In fact, our previous modeling studies with curcumin predicted

this binding site (*34*). However, the inertness of curcumin towards PKCε suggests that either the residues present in the phorbol ester binding cleft in PKCα that are different from PKCε, exert optimum binding to curcumin or the calcium-binding C2 domain of PKCα is responsible for curcumin binding. While studies using a mixture of conventional PKCs, Mahmmoud predicted that curcumin competes with the calcium binding site in C2 domain (*31*), using purified PKCα, Perez-Lara et al discarded this suggestion by showing that PKC modulation, in fact, was dependent on the presence and absence of membrane rather than the calcium concentration (*32*). Also, the activation shown by compounds **2-5,** having long aliphatic chain, suggests the role of lipid membrane in PKC modulation since long aliphatic chain can interact with the membrane lipids. The presence of unsaturated fatty acyl chain in the lipid bilayer greatly influences PKC activity (*53-55*) and in some cases shows isoform preference (*56, 57*). For example, the presence of unsaturation in PC and PS elicits different effects on the activity of PKCα and PKCε (*57*). In terms of phospholipid selectivity, whereas PKCα shows high selectivity for PS (*58*), PKCε shows little selectivity for it (*59*). Now, that curcumin is also known to alter the structure and properties of lipid bilayer (*60-62*), it is highly likely that the affinity of PKCα, PKCε or their complex with curcumin derivatives for plasma membrane would be different. It is also possible that binding of curcumin to PKC affects its interaction with the anchoring protein, RACK in an isoform-dependent manner resulting in translocation variation of PKC isoforms. Taken together, C1 domain residues, lipid membrane and Ca^{++}, and isoform-specific RACK protein, contribute to the different membrane translocation of different PKC isoforms. In this regard, structural studies, specifically a crystal structure of a full-length PKCα complexed with curcumin is expected to shed light on pinpointing the exact site of action of curcumin in PKC.

Our results that the effects of curcumin and its derivatives on PKC is transduced in its downstream readout ERK1/2, either by the Ras →Raf →MEK1/2 →ERK1/2 or the Raf →MEK1/2 →ERK1/2 pathways, these compounds may have therapeutic potential for treating disease states involving PKCα, such as cardiac contractility, atherogenesis, cancer and arterial thrombosis (*63-65*). Since curcumin is a low affinity PKC ligand as compared to phorbol ester or DAG, further structure-activity relationship (SAR) studies on curcumin moiety are required for developing high-affinity curcumin-based PKC ligand.

In conclusion, curcumin and its derivatives show selectivity towards PKCα over PKCε in CHO-K1 cells. The long chain derivatives are less cytotoxic than the parent curcumin and activate PKCα and its downstream target ERK1/2. The hydroxyl group of curcumin is important for modulating its PKC activity. This study shows that simple chemical scaffold like curcumin can be suitably modified to develop isoform selective PKC modulator.

Supporting Information Available.

Absorption and emission maxima of curcumin derivatives; Effect of curcumin derivatives on the membrane translocation of PKCα and PKCε at various concentrations.

Funding Information

This research was supported by the start-up funds from the University of Houston.

Figure Legends

Figure 1: Chemical structure of curcumin **(1)** and its derivatives **(2-6)**

Figure 2: Effect of **1-6** on DPPH radical scavenging activity. Percent of free DPPH (60 μM) in presence of 0.25-60 μM of **1**(●), **2**(■), **3**(▲), **4**(▼), **5**(♦), and **6**(⬣).Values are the average of triplicate experiments and represented as mean ± SEM. Solid lines indicate the Hill fit of dose response curves. The corresponding IC_{50} for **1**, **2**, **3**, **4, and 6** are 14.7±1, 20.8±1, 26.2±1, 25.8±1, and 2.6±1 μM, respectively and the corresponding Hill slopes are 0.96, 0.98, 0.98, 0.99, and 0.97 respectively. Absorbance was measured at 517 nm. For compound **5,** IC_{50} could not be measured.

Figure 3: Effect of **1-6** on CHO-K1 cell viability. The bar graph shows the percentage of viable cells after treatment with a) 0 μM, b) 25 μM, c) 50 μM, d) 100 μM of **1**, **2**, **3**, **4, 5** and **6** for 48 h. Data are expressed as mean ± SD of three independent experiments. Statistical analysis was performed using one-way ANOVA, followed by Bonferroni *post hoc* test. *P< 0.05 compared to control (0 μM). The cell viability was measured by MTT assay.

Figure 4: Effect of **1-6** on the expression of PKCα and PKCε in CHO-K1 cells. Upper panels, Western blot analysis of the whole cell lysate of CHO-K1 after treatment with **1-6** (10 μM) for 24 h. β-actin was used as a reference for equal loading. Control (ctrl) refers to the sample with vehicle (0.1% DMSO) treated cells. Lower panel, bar graph of densitometry analysis of PKC expression, Mean ± SEM, n = 3. Statistical analysis was performed using one-way ANOVA, followed by Bonferroni *post hoc* test.*P <0.05 compared to control.

Figure 5: Effect of curcumin (**1)** on TPA-induced membrane translocation of PKCα and PKCε in CHO-K1 cells. Upper panels, Western blot analysis of the cytosolic (C) and membrane (M) fraction of (**A**) PKCα and (**B**) PKCε after cells either treated with a) 25 μM, b) 12.5 μM, c) 6.25 μM of **1** or co-treated with d) 100 nM of TPA for 1h. Control (ctrl) refers to the sample with vehicle (0.1% DMSO) treated cells. Lower panel, bar graph of densitometry analysis of upper panel immunoblots, Mean ± SEM, n = 3. Statistical analysis was performed using one-way ANOVA, followed by Bonferroni *post hoc* test.*P <0.05 compared to TPA.

Figure 6: Effect of curcumin (**1)** on TPA-induced membrane translocation of endogenous PKCα in CHO-K1 cells. Confocal analysis of PKCα after cells were either treated with **1** (6.25-25 μM) or co-treated with **1** (6.25-25 μM) and TPA (100 nM) for 1 h. 100 nM TPA was used as a positive control. Control (ctrl) refers to the sample with vehicle (0.1% DMSO) treated cells. Images are representative of three independent experiments for each condition. Lower panel, bar graph shows quantification of cytosol to plasma membrane fluorescence intensity ratio of upper panel confocal images, Mean ± SEM, n = 5. Statistical analysis was performed using one-way ANOVA, followed by Bonferroni *post hoc* test.*P <0.05 compared to TPA.

Figure 7: Effect of **1-6** on the membrane translocation of PKCα and PKCε in CHO-K1 cells. Upper panels, Western blot analysis of the cytosolic (C) and the membrane (M) fractions of (**A**) PKCα and (**B**) PKCε after the cells were treated with 10 μM of **1-6** for 24 h. Control (ctrl) refer to the sample with vehicle (0.1% DMSO) treated cells. Lower panel, bar graph of densitometry analysis of upper panel immunoblots, Mean± SEM, n=3. Statistical analysis was performed using one-way ANOVA, followed by Bonferroni *post hoc* test. * P< 0.05 compared to control.

Figure 8: Effect of curcumin **1-4** and **6** on ERK activation in the presence and absence of TPA in CHO-K1 cells. Cells were either treated with 25 μM of **1**(**A**) and **6**(**B**) in presence or absence of

TPA (100 nM) for 1 h or treated with compound **2**-**4** (10 μM) for 24 h (**C**). Control (ctrl) refers to the sample with vehicle treated cells. β actin was used as a reference for equal loading. Lower panel, bar graph of densitometry analysis of upper panel immunoblots, Mean ± SEM, n = 3. Statistical analysis was performed using two-way RM-ANOVA with a *post hoc* Bonferroni test.*P <0.01 compared to control and **P<0.05 compared to control

References

1. Battaini, F., and Mochly-Rosen, D. (2007) Happy birthday protein kinase C: past, present and future of a superfamily, *Pharmacol. Res. 55*, 461-466.
2. Koivunen, J., Aaltonen, V., and Peltonen, J. (2006) Protein kinase C (PKC) family in cancer progression, *Cancer Lett. 235*, 1-10.
3. Griner, E. M., and Kazanietz, M. G. (2007) Protein kinase C and other diacylglycerol effectors in cancer, *Nat. Rev. Cancer 7*, 281-294.
4. Das Evcimen, N., and King, G. L. (2007) The role of protein kinase C activation and the vascular complications of diabetes, *Pharmacol. Res. 55*, 498-510.
5. Bright, R., and Mochly-Rosen, D. (2005) The role of protein kinase C in cerebral ischemic and reperfusion injury, *Stroke 36*, 2781-2790.
6. Chou, W. H., and Messing, R. O. (2005) Protein kinase C isozymes in stroke, *Trends Cardiovasc. Med. 15*, 47-51.
7. Sabri, A., and Steinberg, S. F. (2003) Protein kinase C isoform-selective signals that lead to cardiac hypertrophy and the progression of heart failure, *Mol. Cell. Biochem. 251*, 97-101.
8. Alkon, D. L., Sun, M. K., and Nelson, T. J. (2007) PKC signaling deficits: a mechanistic hypothesis for the origins of Alzheimer's disease, *Trends Pharmacol. Sci. 28*, 51-60.
9. Hofmann, J. (2004) Protein kinase C isozymes as potential targets for anticancer therapy, *Curr. Cancer Drug Targets 4*, 125-146.
10. Mochly-Rosen, D., Das, K., and Grimes, K. V. (2012) Protein kinase C, an elusive therapeutic target? *Nat. Rev. Drug Discov. 11*, 937-957.
11. Newton, A. C. (2001) Protein kinase C: structural and spatial regulation by phosphorylation, cofactors, and macromolecular interactions, *Chem. Rev. 101*, 2353-2364.
12. Nishizuka, Y. (1992) Intracellular signaling by hydrolysis of phospholipids and activation of protein kinase C, *Science 258*, 607-614.
13. Colon-Gonzalez, F., and Kazanietz, M. G. (2006) C1 domains exposed: from diacylglycerol binding to protein-protein interactions, *Biochim. Biophys. Acta 1761*, 827-837.
14. Yang, C., and Kazanietz, M. G. (2003) Divergence and complexities in DAG signaling: looking beyond PKC, *Trends Pharmacol. Sci. 24*, 602-608.
15. Sharkey, N. A., and Blumberg, P. M. (1986) Comparison of the activity of phorbol 12-myristate 13-acetate and the diglyceride glycerol 1-myristate 2-acetate, *Carcinogenesis 7*, 677-679.

16. Kazanietz, M. G., Krausz, K. W., and Blumberg, P. M. (1992) Differential irreversible insertion of protein kinase C into phospholipid vesicles by phorbol esters and related activators, *J. Biol. Chem. 267*, 20878-20886.
17. Boije af Gennas, G., Talman, V., Yli-Kauhaluoma, J., Tuominen, R. K., and Ekokoski, E. (2011) Current status and future prospects of c1 domain ligands as drug candidates, *Curr. Top. Med. Chem. 11*, 1370-1392.
18. Blumberg, P. M., Kedei, N., Lewin, N. E., Yang, D., Czifra, G., Pu, Y., Peach, M. L., and Marquez, V. E. (2008) Wealth of opportunity - the C1 domain as a target for drug development, *Curr. Drug Targets 9*, 641-652.
19. Goel, A., and Aggarwal, B. B. (2010) Curcumin, the golden spice from Indian saffron, is a chemosensitizer and radiosensitizer for tumors and chemoprotector and radioprotector for normal organs, *Nutr. Cancer 62*, 919-930.
20. Epstein, J., Sanderson, I. R., and Macdonald, T. T. (2010) Curcumin as a therapeutic agent: the evidence from in vitro, animal and human studies, *Br. J. Nutr. 103*, 1545-1557.
21. Singh, S. (2007) From exotic spice to modern drug? *Cell 130*, 765-768.
22. Ataie, A., Sabetkasaei, M., Haghparast, A., Moghaddam, A. H., Ataee, R., and Moghaddam, S. N. (2010) Curcumin exerts neuroprotective effects against homocysteine intracerebroventricular injection-induced cognitive impairment and oxidative stress in rat brain, *J. Med. Food 13*, 821-826.
23. Cemil, B., Topuz, K., Demircan, M. N., Kurt, G., Tun, K., Kutlay, M., Ipcioglu, O., and Kucukodaci, Z. (2010) Curcumin improves early functional results after experimental spinal cord injury, *Acta Neurochir. (Wien) 152*, 1583-1590; discussion 1590.
24. Morimoto, T., Sunagawa, Y., Fujita, M., and Hasegawa, K. (2010) Novel heart failure therapy targeting transcriptional pathway in cardiomyocytes by a natural compound, curcumin, *Circ. J. 74*, 1059-1066.
25. Lin, J. K., Chen, Y. C., Huang, Y. T., and Lin-Shiau, S. Y. (1997) Suppression of protein kinase C and nuclear oncogene expression as possible molecular mechanisms of cancer chemoprevention by apigenin and curcumin, *J. Cell. Biochem. Suppl 28-29*, 39-48.
26. Rungseesantivanon, S., Thenchaisri, N., Ruangvejvorachai, P., and Patumraj, S. (2010) Curcumin supplementation could improve diabetes-induced endothelial dysfunction associated with decreased vascular superoxide production and PKC inhibition, *BMC Complement Altern. Med. 10*, 57.
27. Lin, J. K. (2007) Molecular targets of curcumin, *Adv. Exp. Med. Biol. 595*, 227-243.
28. Balasubramanyam, M., Koteswari, A. A., Kumar, R. S., Monickaraj, S. F., Maheswari, J. U., and Mohan, V. (2003) Curcumin-induced inhibition of cellular reactive oxygen species generation: novel therapeutic implications, *J. Biosci. 28*, 715-721.
29. Liu, J. Y., Lin, S. J., and Lin, J. K. (1993) Inhibitory effects of curcumin on protein kinase C activity induced by 12-O-tetradecanoyl-phorbol-13-acetate in NIH 3T3 cells, *Carcinogenesis 14*, 857-861.
30. Reddy, S., and Aggarwal, B. B. (1994) Curcumin is a non-competitive and selective inhibitor of phosphorylase kinase, *FEBS Lett. 341*, 19-22.
31. Mahmmoud, Y. A. (2007) Modulation of protein kinase C by curcumin; inhibition and activation switched by calcium ions, *Br. J. Pharmacol. 150*, 200-208.
32. Perez-Lara, A., Corbalan-Garcia, S., and Gomez-Fernandez, J. C. (2011) Curcumin modulates PKCalpha activity by a membrane-dependent effect, *Arch. Biochem. Biophys. 513*, 36-41.

33. Garg, R., Ramchandani, A. G., and Maru, G. B. (2008) Curcumin decreases 12-O-tetradecanoylphorbol-13-acetate-induced protein kinase C translocation to modulate downstream targets in mouse skin, *Carcinogenesis 29*, 1249-1257.
34. Majhi, A., Rahman, G. M., Panchal, S., and Das, J. (2010) Binding of curcumin and its long chain derivatives to the activator binding domain of novel protein kinase C, *Bioorg. Med. Chem. 18*, 1591-1598.
35. Das, J., Pany, S., Panchal, S., Majhi, A., and Rahman, G. M. (2011) Binding of isoxazole and pyrazole derivatives of curcumin with the activator binding domain of novel protein kinase C, *Bioorg. Med. Chem. 19*, 6196-6202.
36. Pany, S., Majhi, A., and Das, J. (2012) PKC activation by resveratrol derivatives with unsaturated aliphatic chain, *PLoS One 7*, e52888.
37. Nguyen, T. V., Poole, D. P., Harvey, J. R., Stebbing, M. J., and Furness, J. B. (2005) Investigation of PKC isoform-specific translocation and targeting of the current of the late afterhyperpolarizing potential of myenteric AH neurons, *Eur. J. Neurosci. 21*, 905-913.
38. Leterrier, C., Bonnard, D., Carrel, D., Rossier, J., and Lenkei, Z. (2004) Constitutive endocytic cycle of the CB1 cannabinoid receptor, *J. Biol. Chem 279*, 36013-36021.
39. Ferrari, E., Pignedoli, F., Imbriano, C., Marverti, G., Basile, V., Venturi, E., and Saladini, M. (2011) Newly synthesized curcumin derivatives: crosstalk between chemico-physical properties and biological activity, *J. Med. Chem. 54*, 8066-8077.
40. Wilken, R., Veena, M. S., Wang, M. B., and Srivatsan, E. S. (2011) Curcumin: A review of anti-cancer properties and therapeutic activity in head and neck squamous cell carcinoma, *Mol. Cancer 10*, 12.
41. Hossain, D. S., Bhattacharyya, S., Das, T., and Sa, G. (2012) Curcumin: The multi-targeted therapy for cancer regression, *Front. Biosci. (Schol Ed) 4*, 335-355.
42. Jiang, M. C., Yang-Yen, H. F., Yen, J. J., and Lin, J. K. (1996) Curcumin induces apoptosis in immortalized NIH 3T3 and malignant cancer cell lines, *Nutr. Cancer 26*, 111-120.
43. Das, J., and Rahman, G. M. (2014) C1 domains: structure and ligand-binding properties, *Chem. Rev. 114*, 12108-12131.
44. Endo, Y., Yamaguchi, M., Hirano, M., and Shudo, K. (1996) Role of hydrophobic moiety of tumor promoters. Synthesis and activity of 9-alkylated banzolactams, *Chem. Pharm. Bull. 44*, 1138-1140.
45. Endo, Y., and Yokoyama, A. (2000) Role of the hydrophobic moiety of tumor promoters. Synthesis and activity of 2-alkylated benzolactams, *Bioorg. Med. Chem. Lett. 10*, 63-66.
46. Das, J., Pany, S., and Majhi, A. (2011) Chemical modifications of resveratrol for improved protein kinase C alpha activity, *Bioorg. Med. Chem. 19*, 5321-5333.
47. Shirai, Y., Kashiwagi, K., Yagi, K., Sakai, N., and Saito, N. (1998) Distinct effects of fatty acids on translocation of gamma- and epsilon-subspecies of protein kinase C, *J. Cell. Biol. 143*, 511-521.
48. Zhang, Q., Zhong, Y., Yan, L. N., Sun, X., Gong, T., and Zhang, Z. R. (2011) Synthesis and preliminary evaluation of curcumin analogues as cytotoxic agents, *Bioorg. Med. Chem. Lett. 21*, 1010-1014.
49. Adams, B. K., Ferstl, E. M., Davis, M. C., Herold, M., Kurtkaya, S., Camalier, R. F., Hollingshead, M. G., Kaur, G., Sausville, E. A., Rickles, F. R., Snyder, J. P., Liotta, D.

C., and Shoji, M. (2004) Synthesis and biological evaluation of novel curcumin analogs as anti-cancer and anti-angiogenesis agents, *Bioorg. Med. Chem. 12*, 3871-3883.
50. Hansch, C., Bonavida, B., Jazirehi, A. R., Cohen, J. J., Milliron, C., and Kurup, A. (2003) Quantitative structure–Activity relationships of phenolic compounds causing apoptosis, *Bioorg. Med. Chem. 11*, 617-620.
51. Fujisawa, S., Atsumi, T., Ishihara, M., and Kadoma, Y. (2004) Cytotoxicity, ROS-generation activity and radical-scavenging activity of curcumin and related compounds, *Anticancer Res. 24*, 563-569.
52. Priyadarsini, K. I., Maity, D. K., Naik, G. H., Kumar, M. S., Unnikrishnan, M. K., Satav, J. G., and Mohan, H. (2003) Role of phenolic O-H and methylene hydrogen on the free radical reactions and antioxidant activity of curcumin, *Free Rad. Biol. Med. 35*, 475-484.
53. Stubbs, C. D., and Slater, S. J. (1996) The effects of non-lamellar forming lipids on membrane protein-lipid interactions, *Chem. Phys. Lipids 81*, 185-195.
54. Goldberg, E. M., and Zidovetzki, R. (1997) Effects of dipalmitoylglycerol and fatty acids on membrane structure and protein kinase C activity, *Biophys. J. 73*, 2603-2614.
55. Giorgione, J. R., Kraayenhof, R., and Epand, R. M. (1998) Interfacial membrane properties modulate protein kinase C activation: role of the position of acyl chain unsaturation, *Biochemistry 37*, 10956-10960.
56. O'Flaherty, J. T., Chadwell, B. A., Kearns, M. W., Sergeant, S., and Daniel, L. W. (2001) Protein kinases C translocation responses to low concentrations of arachidonic acid, *J. Biol. Chem. 276*, 24743-24750.
57. Slater, S. J., Kelly, M. B., Yeager, M. D., Larkin, J., Ho, C., and Stubbs, C. D. (1996) Polyunsaturation in cell membranes and lipid bilayers and its effects on membrane proteins, *Lipids 31 Suppl.*, S189-192.
58. Medkova, M., and Cho, W. (1998) Differential membrane-binding and activation mechanisms of protein kinase C-alpha and -epsilon, *Biochemistry 37*, 4892-4900.
59. Stahelin, R. V., Digman, M. A., Medkova, M., Ananthanarayanan, B., Melowic, H. R., Rafter, J. D., and Cho, W. (2005) Diacylglycerol-induced membrane targeting and activation of protein kinase Cepsilon: mechanistic differences between protein kinases Cdelta and Cepsilon, *J. Biol. Chem. 280*, 19784-19793.
60. Hung, W. C., Chen, F. Y., Lee, C. C., Sun, Y., Lee, M. T., and Huang, H. W. (2008) Membrane-thinning effect of curcumin, *Biophys. J. 94*, 4331-4338.
61. Barry, J., Fritz, M., Brender, J. R., Smith, P. E., Lee, D. K., and Ramamoorthy, A. (2009) Determining the effects of lipophilic drugs on membrane structure by solid-state NMR spectroscopy: the case of the antioxidant curcumin, *J. Am. Chem. Soc. 131*, 4490-4498.
62. Perez-Lara, A., Ausili, A., Aranda, F. J., de Godos, A., Torrecillas, A., Corbalan-Garcia, S., and Gomez-Fernandez, J. C. (2010) Curcumin disorders 1,2-dipalmitoyl-sn-glycero-3-phosphocholine membranes and favors the formation of nonlamellar structures by 1,2-dielaidoyl-sn-glycero-3-phosphoethanolamine, *J. Phys.Chem. B 114*, 9778-9786.
63. Nakashima, S. (2002) Protein kinase C alpha (PKC alpha): regulation and biological function, *J. Biochem. 132*, 669-675.
64. Liu, Q., and Molkentin, J. D. (2011) Protein kinase Calpha as a heart failure therapeutic target, *J. Mol. Cell. Cardiol. 51*, 474-478.
65. Teicher, B. A. (2006) Protein kinase C as a therapeutic target, *Clin. Cancer Res. 12*, 5336-5345.

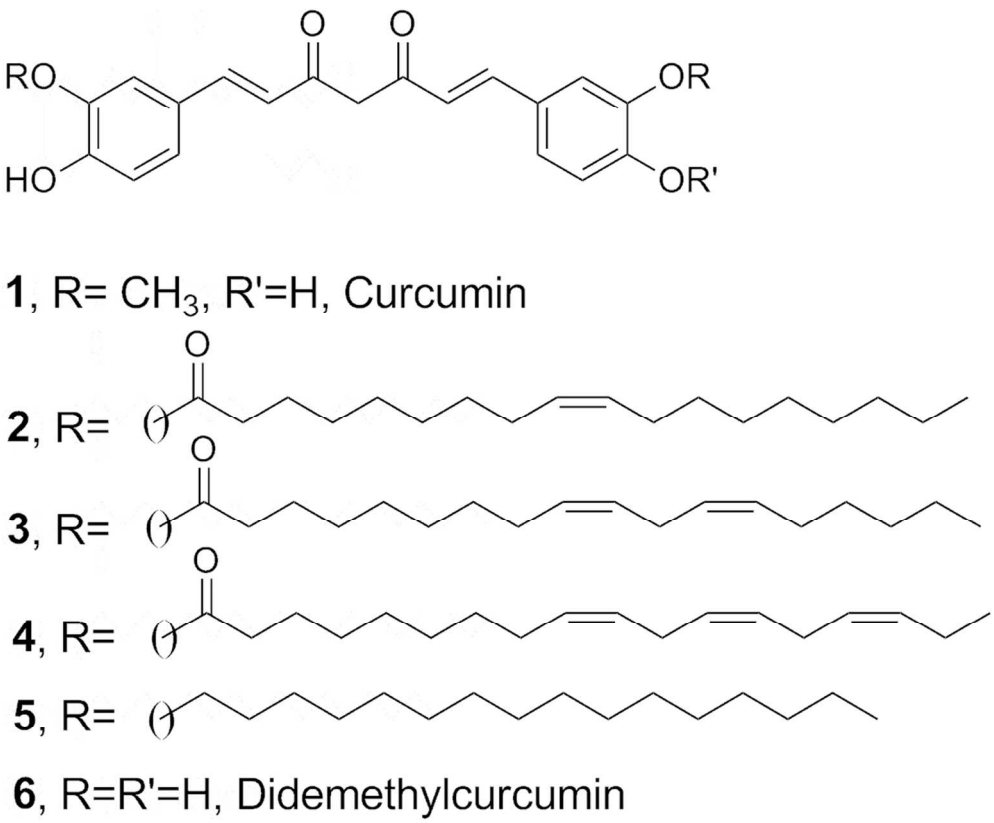

Figure 1: Chemical structure of curcumin (1) and its derivatives (2-6)
98x80mm (300 x 300 DPI)

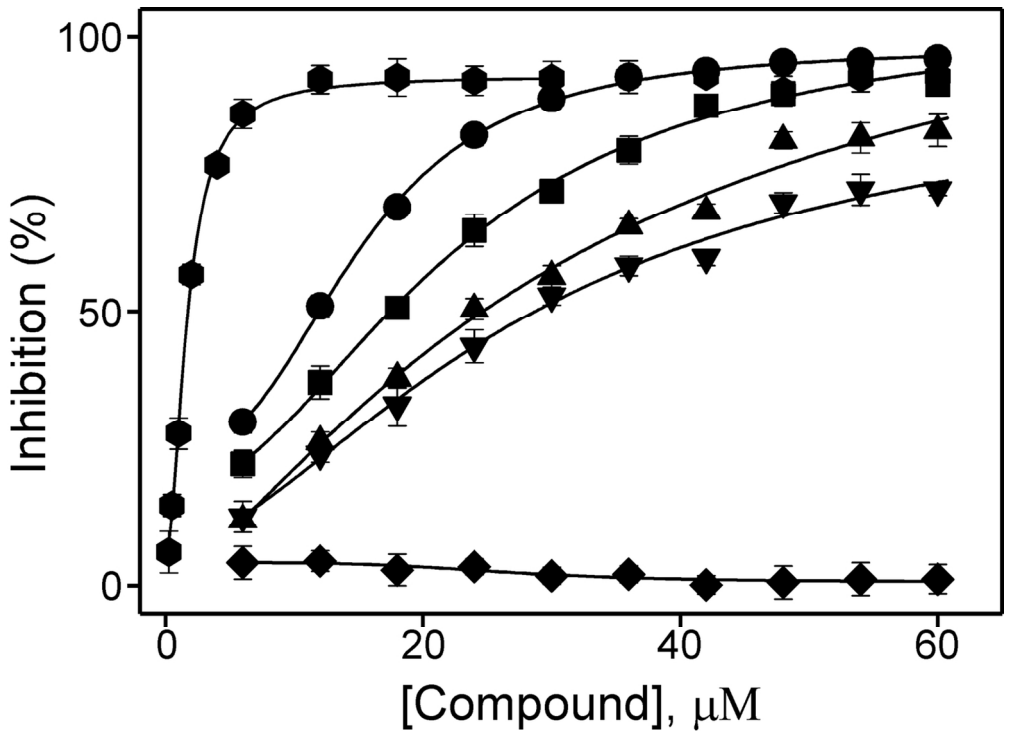

Figure 2: Effect of 1-6 on DPPH radical scavenging activity. Percent of free DPPH (60 μM) in presence of 0.25-60 μM of 1(●), 2(■), 3(▲), 4(▼), 5(♦), and 6( ).Values are the average of triplicate experiments and represented as mean ± SEM. Solid lines indicate the Hill fit of dose response curves. The corresponding IC50 for 1, 2, 3, 4, and 6 are 14.7±1, 20.8±1, 26.2±1, 25.8±1, and 2.6±1 μM, respectively and the corresponding Hill slopes are 0.96, 0.98, 0.98, 0.99, and 0.97 respectively. Absorbance was measured at 517 nm. For compound 5, IC50 could not be measured.
63x45mm (600 x 600 DPI)

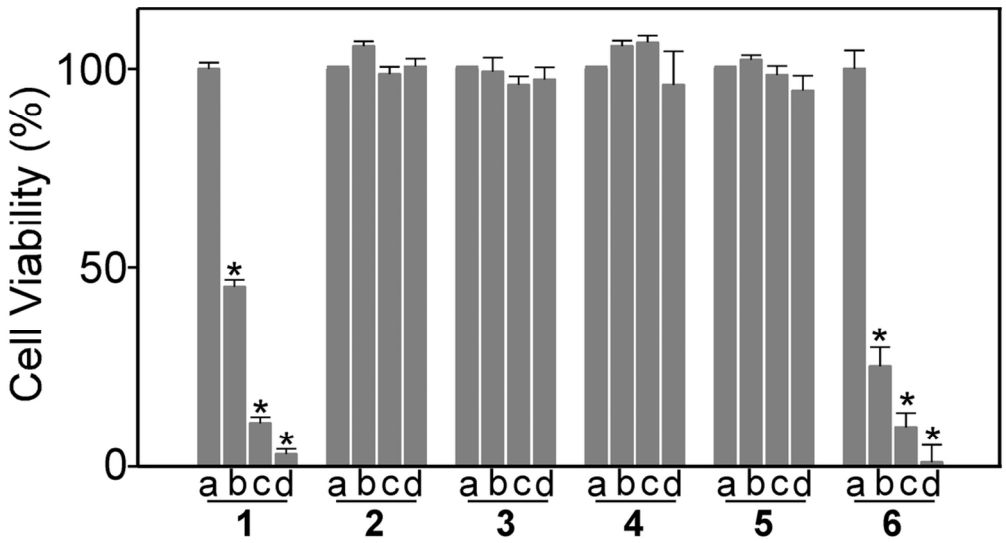

Figure 3: Effect of 1-6 on CHO-K1 cell viability. The bar graph shows the percentage of viable cells after treatment with a) 0 μM, b) 25 μM, c) 50 μM, d) 100 μM of 1, 2, 3, 4, 5 and 6 for 48 h. Data are expressed as mean ± SD of three independent experiments. Statistical analysis was performed using one-way ANOVA, followed by Bonferroni post hoc test. *P< 0.05 compared to control (0 μM). The cell viability was measured by MTT assay.
51x27mm (600 x 600 DPI)

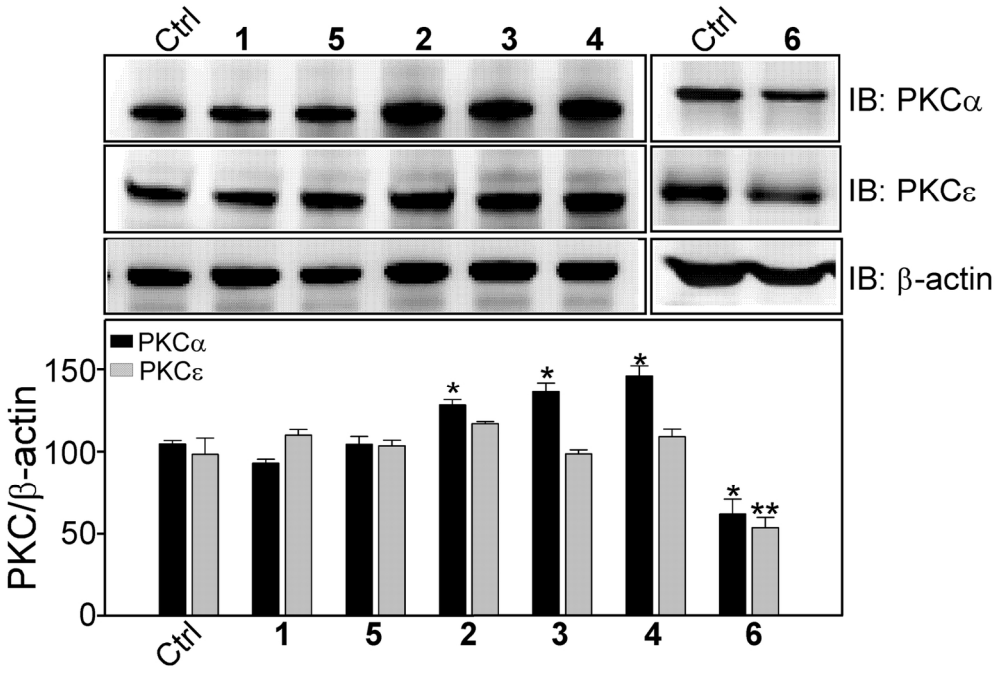

Figure 4: Effect of 1-6 on the expression of PKCα and PKCε in CHO-K1 cells. Upper panels, Western blot analysis of the whole cell lysate of CHO-K1 after treatment with 1-6 (10 μM) for 24 h. β-actin was used as a reference for equal loading. Control (ctrl) refers to the sample with vehicle (0.1% DMSO) treated cells. Lower panel, bar graph of densitometry analysis of PKC expression, Mean ± SEM, n = 3. Statistical analysis was performed using one-way ANOVA, followed by Bonferroni post hoc test.*P <0.05 compared to control.
74x50mm (600 x 600 DPI)

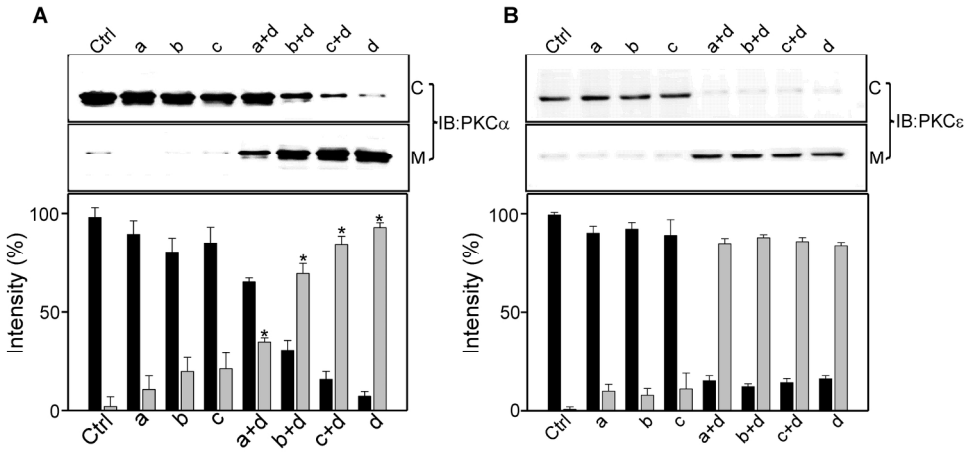

Figure 5: Effect of curcumin (1) on TPA-induced membrane translocation of PKCα and PKCε in CHO-K1 cells. Upper panels, Western blot analysis of the cytosolic (C) and membrane (M) fraction of (A) PKCα and (B) PKCε after cells either treated with a) 25 μM, b) 12.5 μM, c) 6.25 μM of 1 or co-treated with d) 100 nM of TPA for 1h. Control (ctrl) refers to the sample with vehicle (0.1% DMSO) treated cells. Lower panel, bar graph of densitometry analysis of upper panel immunoblots, Mean ± SEM, n = 3. Statistical analysis was performed using one-way ANOVA, followed by Bonferroni post hoc test.*P <0.05 compared to TPA.
95x47mm (600 x 600 DPI)

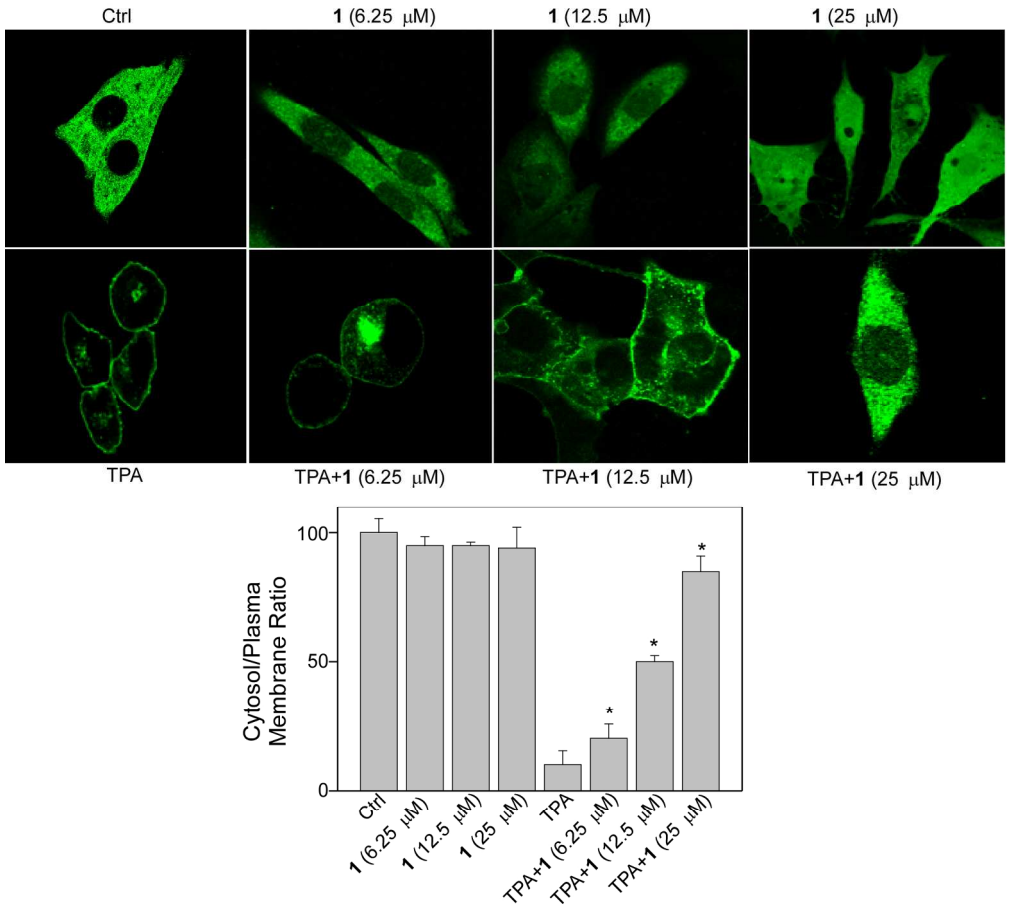

Figure 6: Effect of curcumin (1) on TPA-induced membrane translocation of endogenous PKCα in CHO-K1 cells. Confocal analysis of PKCα after cells were either treated with 1 (6.25-25 μM) or co-treated with 1 (6.25-25 μM) and TPA (100 nM) for 1 h. 100 nM TPA was used as a positive control. Control (ctrl) refers to the sample with vehicle (0.1% DMSO) treated cells. Images are representative of three independent experiments for each condition. Lower panel, bar graph shows quantification of cytosol to plasma membrane fluorescence intensity ratio of upper panel confocal images, Mean ± SEM, n = 5. Statistical analysis was performed using one-way ANOVA, followed by Bonferroni post hoc test.*P <0.05 compared to TPA.
183x166mm (300 x 300 DPI)

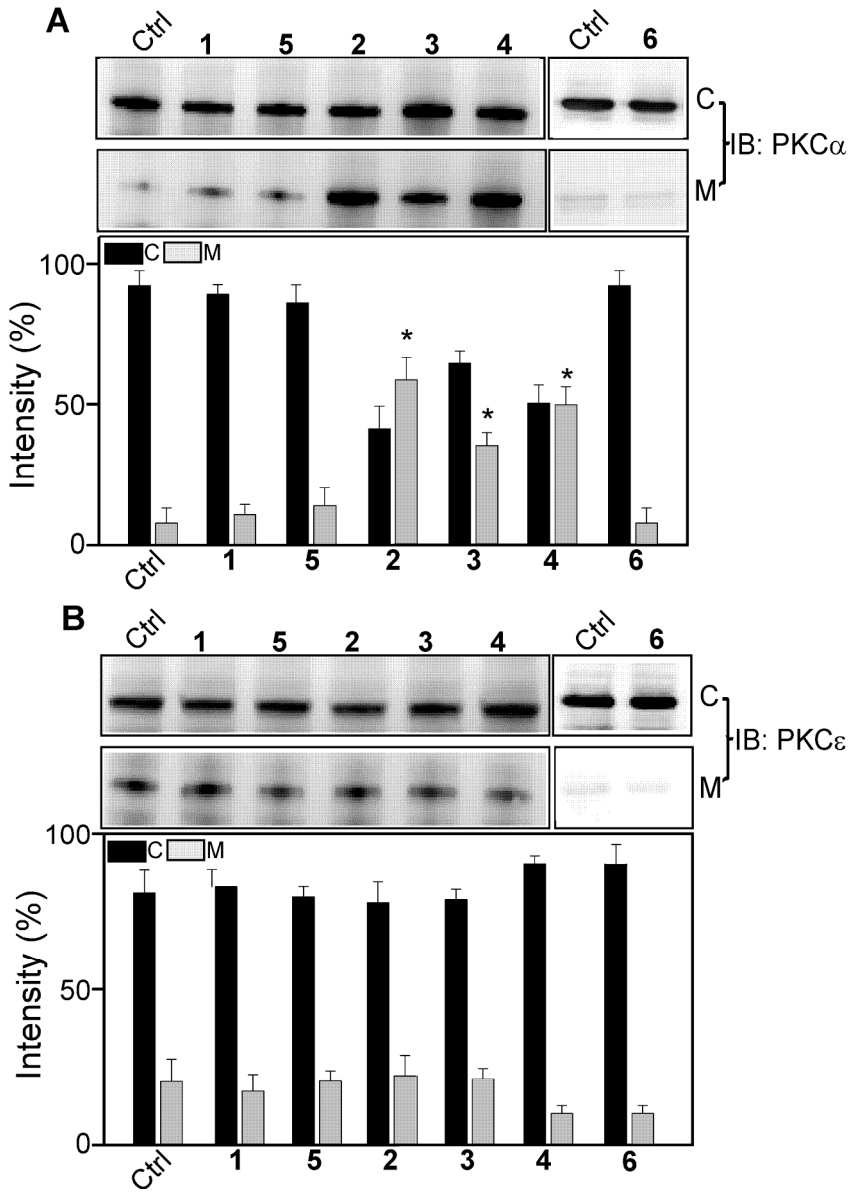

Figure 7: Effect of 1-6 on the membrane translocation of PKCα and PKCε in CHO-K1 cells. Upper panels, Western blot analysis of the cytosolic (C) and the membrane (M) fractions of (A) PKCα and (B) PKCε after the cells were treated with 10 μM of 1-6 for 24 h. Control (ctrl) refer to the sample with vehicle (0.1% DMSO) treated cells. Lower panel, bar graph of densitometry analysis of upper panel immunoblots, Mean± SEM, n=3. Statistical analysis was performed using one-way ANOVA, followed by Bonferroni post hoc test. * P< 0.05 compared to control.
149x211mm (600 x 600 DPI)

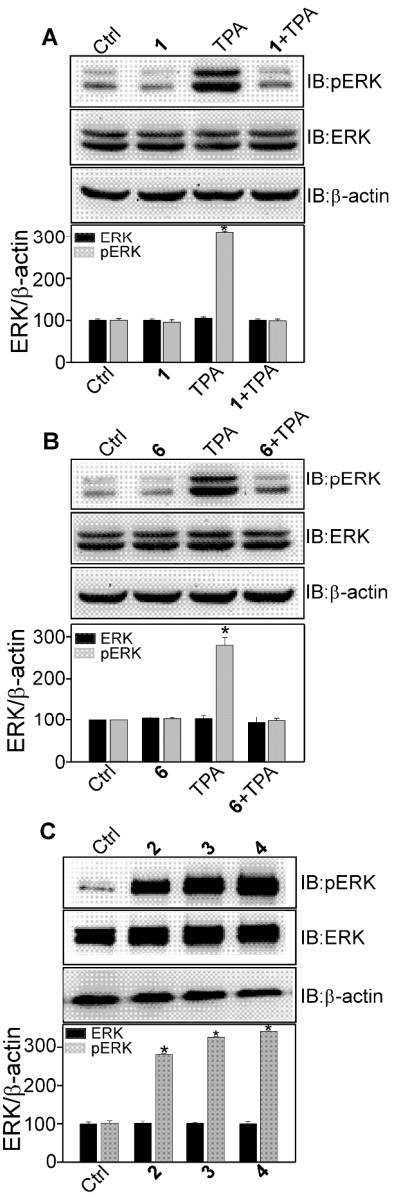

Figure 8: Effect of curcumin 1-4 and 6 on ERK activation in the presence and absence of TPA in CHO-K1 cells. Cells were either treated with 25 μM of 1(A) and 6(B) in presence or absence of TPA (100 nM) for 1 hr or treated with compound 2-4 (10 μM) for 24 h (C). Control (ctrl) refers to the sample with vehicle treated cells. β actin was used as a reference for equal loading. Lower panel, bar graph of densitometry analysis of upper panel immunoblots, Mean ± SEM, n = 3. Statistical analysis was performed using two-way RM-ANOVA with a post hoc Bonferroni test.*P <0.01 compared to control and **P<0.05 compared to control
216x660mm (600 x 600 DPI)

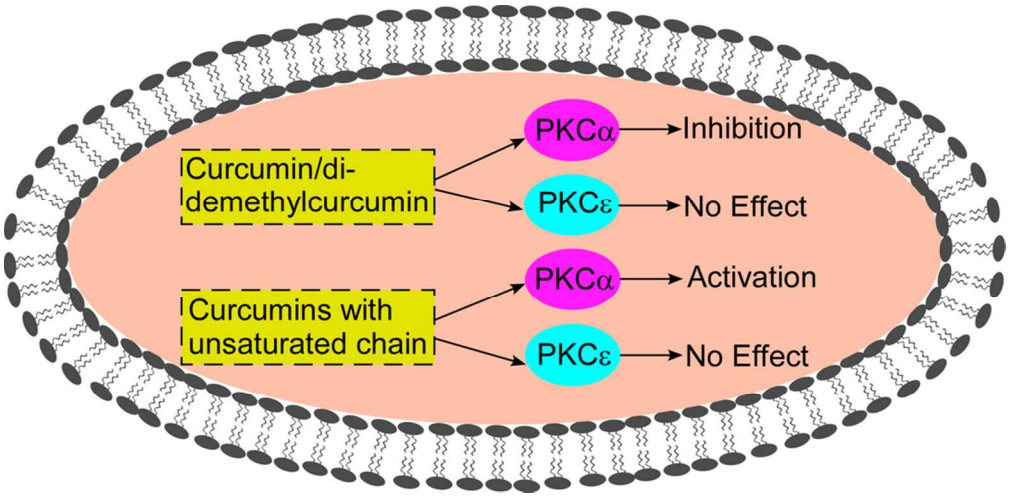

Table of Contents graphic
45x22mm (600 x 600 DPI)